Available online at www.sciencedirect.com
ScienceDirect
Catalysis Today 122 (2007) 248–253
CATALYSIS TODAY
www.elsevier.com/locate/cattod

Magnetron sputtering of gold nanoparticles onto WO_3 and activated carbon

Gabriel M. Veith [a,*], Andrew R. Lupini [a], Stephen J. Pennycook [a], Alberto Villa [b], Laura Prati [b], Nancy J. Dudney [a]

[a] *Materials Science and Technology Division, Oak Ridge National Laboratory, Oak Ridge, TN 37831, USA*
[b] *Dipartimento di Chimica Inorganica, Metallorganica è Analitica, Universita' di Milano, via Venezian 21 20133 Milano, Italy*

Available online 17 January 2007

Abstract

In this paper we describe the production and investigation of two supported gold catalyst systems prepared by magnetron sputtering: Au on WO_3 and Au on activated carbon. The magnetron sputtering technique entails using an argon plasma to sputter a high purity gold target producing a flux of gold atoms which are deposited onto a constantly tumbling support material. This technique offers a number of advantages over conventional chemical preparation methods. One advantage is the ability to create gold nanoparticles (diameters <3 nm) on unusual support materials, such as WO_3 and carbon, which are generally not accessible using the ubiquitous deposition-precipitation technique. We present data demonstrating the formation of catalytic gold nanoparticles with average diameters of 1.7 nm (Au/C) and 2.1 nm (Au/WO_3), as well as a substantial number of single atom species on the Au/C sample. Prototypical carbon monoxide oxidation (Au/WO_3) and glycerol oxidation (Au/C) reactions were performed in order to gauge the activity of these catalysts. The WO_3 supported catalyst exhibits substantial catalytic activity from room temperature to 135 °C (0.0018–0.082 mol CO/mol Au s) with an activation energy near 23 kJ/mol. The activity of the Au/C catalyst was compared to a Au/C catalyst prepared from a poly(vinyl alcohol) (PVA) sol. The smaller catalysts prepared by sputtering are more active than the large gold particles prepared using the PVA sol, however the larger gold nanoparticles are substantially more selective towards the production of intermediate products from the oxidation of glycerol.
Published by Elsevier B.V.

Keywords: Sputtering; Gold catalyst; Acidic support; Glycerol oxidation; Aberration corrected; Scanning Transmission Electron Microscopy

1. Introduction

The origin of the surprisingly large catalytic activity reported for supported gold catalysts has been the subject of intense debate within the literature. There are many experimental and theoretical papers demonstrating that various parameters affect the activity of the catalysts including: particle size, particle shape, support material, synthesis technique, and treatment conditions [1–5]. However, definitive studies elucidating why or how these parameters affect activity are lacking. Catalyst studies to help resolve these issues have been hampered by poor synthetic reproducibility [6] and the large variations in synthesis routes.

One of the most common methods used for the preparation of supported gold nanoparticles is the deposition-precipitation (DP) technique [7]. With proper control of the pH, temperature, and concentration of gold in solution, gold hydroxide is deposited onto the support material [7]. This catalyst precursor is washed, dried, and annealed to form small (<5 nm), fairly uniform catalyst particles [8]. The DP method works well, in that it produces highly active catalysts, but there are a number problems with this method. These problems include the incomplete transfer of the gold from solution to the support, the wide variety of conditions that affect the final product (succinctly summarized by Moreau et al. [8]), and most importantly, the limited nature of candidate support materials. For example, DP cannot produce Au particles, with diameters less than 5 nm, on support materials with low isoelectric points, like SiO_2 and WO_3 [2].

One of the most active topics of discussion in the literature concerns the role the support material plays in the catalytic reactions. For reactions such as ethylene glycol oxidation, the surface properties of the support carbon were found to affect the

* Corresponding author. Tel.: +1 865 576 0027.
E-mail address: veithgm@ornl.gov (G.M. Veith).

0920-5861/$ – see front matter. Published by Elsevier B.V.
doi:10.1016/j.cattod.2007.01.010

activity of the gold catalysts [9]. Supports used for carbon monoxide oxidation catalysts were also found to have an effect on the rate of reaction [10]. These supports are generally divided into two classes: active and inactive supports. Active supports are relatively easily reduced (TiO_2, CeO_2, and Fe_2O_3) and could provide a reservoir or storage for oxygen; whereas ''inactive'' supports (SiO_2, Al_2O_3, and ZrO_2) are generally not as easily reduced [10]. It is widely reported that catalysts on ''active'' supports exhibit higher catalytic activity than those on ''inactive'' supports [10], though there have been reports of Au/Al_2O_3 catalysts with activity matching or exceeding Au/TiO_2 [11,12].

In order to investigate supports not accessible by solution techniques, we are developing a new synthetic procedure based on the physical vapor deposition technique of magnetron sputtering. This method entails the sputtering of a high purity gold metal target with an argon ion plasma and the subsequent deposition of gold onto a support material. The support material is constantly tumbling, resulting in a fresh surface for the gold to deposit onto. After the deposition, no further treatment is required, such as washing, annealing or processing aqueous waste, making it a truly one step procedure to prepare bulk catalysts. Since the gold target is pure metal, there is no residual chloride ion contamination resulting in an inherently cleaner catalyst surface. Furthermore, since we are not using solutions, we are not limited by the substrate's isoelectric point.

This paper reports the synthesis and preliminary characterization of two catalyst systems: Au supported on WO_3 and Au supported on activated carbon. We chose these two systems in order to demonstrate the wide variety of catalysts that can be produced by this technique. WO_3 is a reducible, narrow band gap oxide like TiO_2. Investigating this support material may help provide insight into how the surface acidity of an ''active'' support affects the catalytic oxidation of CO. The isoelectric point of WO_3 is substantially less than 1, compared to 4.5–6 for TiO_2, making it impossible to apply DP to prepare Au catalysts on this support [13,14]. The second system investigated in this work was gold supported on activated carbon. There are a number of reasons for selecting carbon as a catalyst support, including stability in acidic or basic environments and ease of catalyst recycling. From a fundamental perspective, carbon is almost the ideal support for microscopy studies due to its low atomic number. This catalyst was evaluated for the oxidation of glycerol [15,16].

2. Experimental

In a large vacuum chamber, a 2-in. diameter (5.1 cm) magnetron sputter source was positioned 12 cm above a stainless steel (SS) cup, tilted 45° from vertical. A second smaller SS cup was placed inside the larger SS cup. The support powders were placed in the smaller cup along with two 2.54 cm Teflon stir bars. The SS cups were rotated at 43 revolutions per minute using a vacuum compatible stepper motor. This rotation causes the support powders to tumble and constantly randomize, exposing a new surface to the sputter source. The Teflon stir bars were used to promote mixing of the powders as they tumbled. A schematic of the deposition set up and additional experimental details are presented in Refs. [17,18].

The support materials consisted of WO_3 (H.C. Stark, >99.6 purity, SA = 5 $m^2\ g^{-1}$) and an activated carbon (X40S from Camel Chemicals, SA = 1100 $m^2\ g^{-1}$, pH 8–9). Approximately 4 g of WO_3 or 1 g of activated carbon were loaded into the cups. At the end of the deposition process, some of the support material was stuck to the side of the inner SS cup, while most of the powder was freely tumbling. In order to collect the powder, the inner SS cup was simply removed and inverted onto a piece of weighing paper. The powder that was stuck to the side remained in the cup and was not used for the subsequent work.

For comparison purposes, a Au/C catalyst was prepared using a previously described poly(vinyl alcohol) (PVA) sol method [19]. Before use, the carbon was pretreated for 12 h in a 6 M HCl solution, and then filtered and washed several times with distilled water until the pH of the wash was between 6 and 6.5. The pretreated carbon was dried for ~6 h at 150 °C in air. An aqueous $HAuCl_4$ solution of 100 μg/mL was prepared by dissolving gold (30 mg, 99.9999% purity, Fluka) in a minimum amount of HCl/HNO_3 3/1 (v/v) mixture. The excess acid was removed by gently heating the gold-aqua regia solution. The $HAuCl_4$ was then diluted with distilled water until the pH was ~2. While vigorously stirring the aqueous auric acid, a 2 wt% PVA solution (0.96 mL, Aldrich, M_W = 10,000) was added, followed by the dropwise addition of a freshly prepared 0.1 M solution of $NaBH_4$ (7.62 mL, Fluka, >96%) to yield a ruby red metallic sol [19].

The gold loading for each catalyst was determined using a Thermo Jarrell Ash IRIS Inductively Coupled Plasma (ICP) Optical Emission Spectrometer. Five mL of freshly prepared aqua regia (3:1 mixture of hydrochloric acid and nitric acid) was used to dissolve the Au from the samples for analysis. The Au/WO_3/aqua-regia mixture was diluted with 18.3 MΩ deionized water and then centrifuged to separated the WO_3 from the acid. This washing was repeated three times. The aqueous portion of the centrifuged solution was collected, then diluted to 50 mL with 18.3 MΩ deionized water. The Au/C sample was weighed and loaded into a homemade NaCl crucible then annealed at 700 °C for 2 h in air to burn off the carbon support. The residue was then dissolved in 5 mL of freshly made aqua-regia and diluted with 18.3 MΩ deionized water. A series of ICP standards were prepared by serial dilution of an Au reference prepared by Alfa-Aesar. The dissolved NaCl had no effect on the ICP data.

A VG Microscopes HB603 UHV STEM operating at 300 kV equipped with an aberration corrector from Nion Co. and a VG microscopes HB501 UHV STEM operating at 100 kV equipped with a Nion Co. aberration corrector were used to image the catalyst samples. The 603 system was used to image the sputtered samples, while the 501 system was used for the Au/C prepared by PVA sol. The 603 system has been shown to have a resolution of better than 0.8 Angstroms [20], although the main reason for using it was the sensitivity available in the high-angle annular dark field (HAADF) imaging mode. This mode provides Z-contrast imaging, where the brightness depends

on the thickness and approximately the square of the atomic number [21,22]. This mode is particularly suitable for investigating carbon supported catalyst samples because even the smallest nanoparticles, including single gold atoms, are visible on real supports that can be up to several nm thick. Gold particles were distinguished from the WO_3 support due to the concentration of heavy gold atoms, although only a limited number of particles could be investigated due to the thickness of the WO_3. Analysis of the WO_3 supported gold particles may underestimate the size of the larger gold nanoparticles, or miss some of the smallest particles because there is less contrast against the heavy support.

The catalytic activity of Au/WO_3 was determined using a custom built flow reactor to monitor the conversion of carbon monoxide to carbon dioxide. 0.15 g of catalyst was loaded into a quartz U-tube (i.d. = 4 mm, bed 14 mm thick) and supported on both ends with glass wool. A mixture of high purity Helium (Air Liquide-99.99%), oxygen (Air Liquide-Ultra High Purity), and carbon monoxide (Research grade, Matheson, stored in an aluminum cylinder) was delivered from three Sierra Instruments Mass Flow valves at rates of 22:2:1 standard cubic centimeters per minute (SCCM), respectively. The product evolution was monitored with a Ametek Dymaxion mass spectrometer (0–200 amu range). Calibration of the mass spectrometer was accomplished with several mixtures of CO and O_2. The sample was heated using a heating mantle attached to a variac device from 20 °C to 135 °C over a 2.5 h period. The temperature of the catalyst bed was determined using a embedded K-type thermocouple. For comparison purposes, a Au/TiO_2 reference catalyst, obtained from the World Gold Council (Lot #02–05), and a blank WO_3 sample were also evaluated under the same test conditions.

Glycerol oxidation was performed at 50 °C using a glass reactor (30 mL capacity), equipped with heater, mechanical stirrer, gas supply system and thermometer. A premade solution (0.3 M with NaOH/glycerol ratio = 4 mol/mol) was added to the reactor and the catalyst (glycerol/gold ratio = 1000 mol/mol) was suspended in the solution. Once the required temperature (50 °C) was reached, the gas supply was switched from a nitrogen purge to three atmospheres of oxygen, and the monitoring of the reaction started. Samples were removed periodically and analysed with a Varian 9010 high performance liquid chromatograph equipped with a Varian 9050 variable wavelength UV–vis detector (210 nm) and a Waters refractive index detector in series. An Alltech OA-1000 column (300 mm × 6.5 mm) was used with an aqueous 0.1% H_3PO_4 solution (0.5 mL/min) as the eluent. Product evolution was determined by comparing the retention times for pure reference samples.

3. Results and discussion

3.1. Au on WO_3

After the deposition, the sample came out of the vacuum chamber a slightly darker shade of green then the native WO_3 support material. ICP results determined that after 4 h and 20 min of deposition, the sample contained 0.52 wt% Au. The WO_3 tumbled quite well, resulting in a recovery rate of 95%.

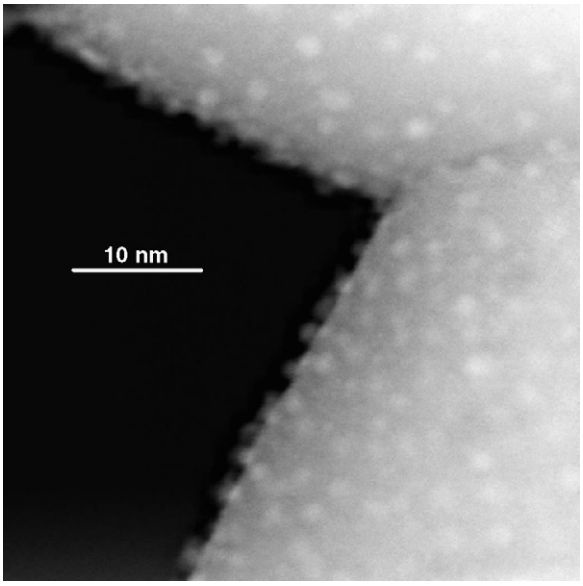

Fig. 1. Z-contrast STEM image of the 0.52 wt% Au on WO_3 sample. The gold nanoparticles are the white spots on the WO_3 surface. The contrast of the small gold particles has been enhanced and the image smoothed, so that small particles are visible, despite the lack of contrast to the background.

Scanning transmission electron microscopy was used to estimate the gold particle sizes. A representative STEM image, enhanced for contrast, is shown in Fig. 1. The image reveals the presence of numerous 2 nm gold particles decorating the surface of the WO_3 support material. Fig. 2 shows a histogram of particle sizes for the Au/WO_3 sample. The histogram and the STEM image reveal that this technique successfully prepared a high concentration of small gold nanoparticles (<2.5 nm) while there are a few larger gold particles (4–6 nm in diameter).

In order to evaluate the activity of the WO_3 supported gold catalyst, we performed a simple carbon monoxide oxidation reaction. Fig. 3 shows a plot of the rate of carbon monoxide conversion (mol CO/mol Au s) versus temperature. At room

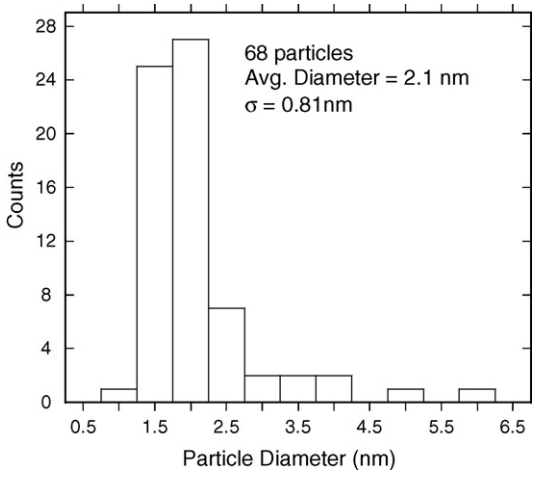

Fig. 2. Particle size histogram for the 0.52 wt% Au on WO_3 sample.

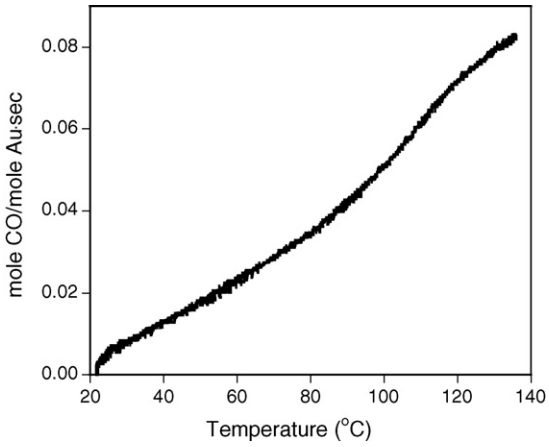

Fig. 3. Plot of catalytic activity (mol CO/mol Au s) versus temperature (°C) from the oxidation of carbon monoxide.

temperature the sample has a conversion rate of 0.0018 mol CO/mol Au s (2% CO conversion). At 135 °C the catalyst has an activity of 0.082 mol CO/mol Au s (48% CO conversion). For comparison, the rate of oxidation for a fresh untreated reference Au–TiO_2 catalyst, under the same gas test conditions, was estimated to be 0.05 mol CO/mol Au s at room temperature or about 28 times more active. Uncoated WO_3 exhibited no catalytic activity towards the oxidation of carbon monoxide up to 180 °C confirming that the observed activity was due to the gold nanoparticles.

As the sample temperature is elevated there is an increase in the reaction rate. The temperature dependence is complex and does not reflect a simple thermal activation. The best fit of the rate between 30 °C and 110 °C as an Arrhenius plot indicates an activation energy of the reaction, E_a, of about 23 kJ/mol. This activation energy is in good agreement with previously reported values for supported gold catalysts [3], though none of the previous reports involve WO_3 as a support. Deviations at high

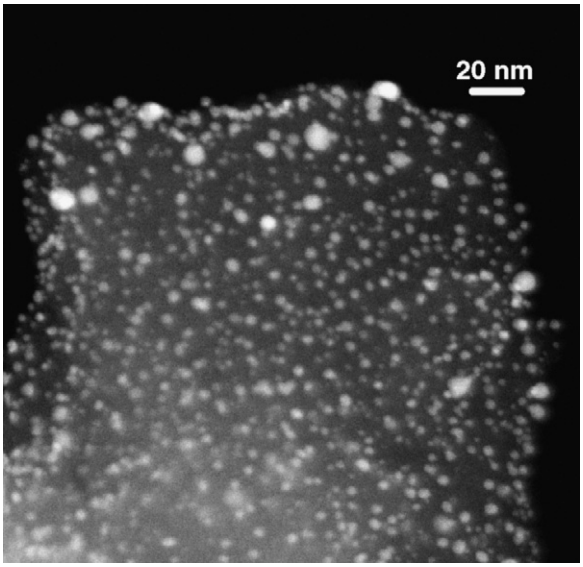

Fig. 4. Z-contrast STEM image of the 0.74 wt% Au on activated carbon sample.

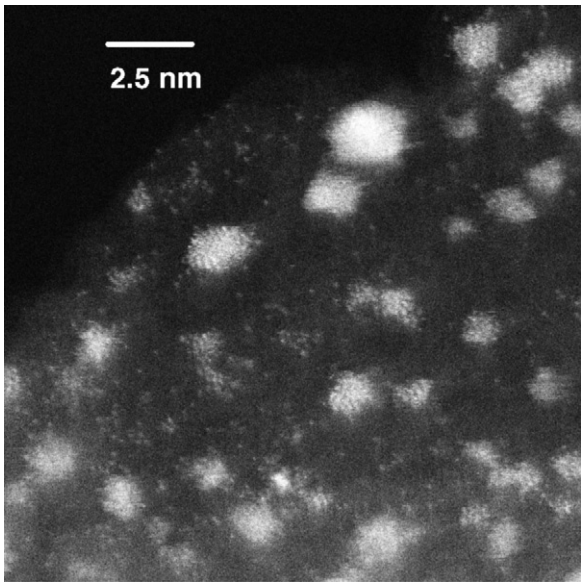

Fig. 5. Z-contrast STEM image of the 0.74 wt% Au on activated carbon. Notice the single gold atoms on the carbon surface.

and low temperatures from such a thermally activated process may be due to mass transport effects [3] or a change in reaction mechanism at higher temperatures. Further studies are needed to address this issue as well as the reaction mechanism.

3.2. Au on activated carbon

A second catalyst sample was prepared by sputtering gold onto a high surface area activated carbon. STEM images for this sample are presented in Figs. 4 and 5. Particle size distributions of the gold nanoparticles are presented in Fig. 6. Several observations can be derived from this data. As Figs. 4 and 6 reveal, we have created a very uniform, almost homogeneous distribution of gold nanoparticles on the surface. The average diameter of the nanoparticles is estimated to be about 1.7 nm. Fig. 5 reveals that in addition to the 1.7 nm gold particles, we have a significant fraction of single gold atoms stabilized and trapped on the surface of the carbon. The presence of single Au

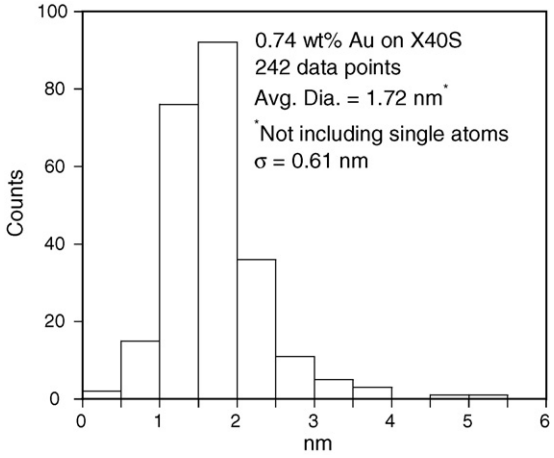

Fig. 6. Particle size histogram of the 0.74 wt% Au on activated carbon sample.

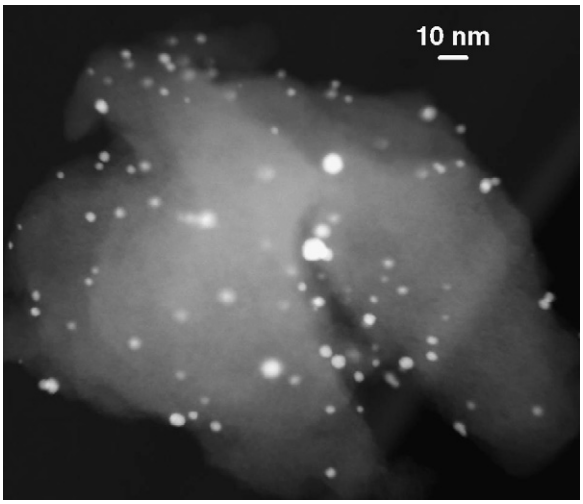

Fig. 7. Z-contrast STEM image of a 0.7 wt% Au on activated carbon prepared using a PVA sol.

atoms on the surface is evidence that the deposition flux is largely atomic or very small clusters (as expected from the process gas pressure). The activated carbon apparently has enough nucleation sites or functionalized surface sites to trap some of these single atoms before they can be incorporated into nanoparticles. These particles are some of the smallest gold particles reported for carbon supports.

For comparison purposes, a 0.70 wt% Au–C sample was prepared by immobilizing a PVA sol and used as a catalyst under the same conditions. Excellent metal dispersion is obtained by using the preformed gold sol described above; whereas previous work, where deposition precipitation was used, reported the formation of large aggregates of gold particles on activated carbon [19]. A representative STEM image of the PVA–Au/C sample is shown in Fig. 7. The gold particles in this sample had an average diameter of 6.9 nm, determined from STEM data, Fig. 8.

In order to examine the activity of the Au/C catalysts, we performed a liquid phase glycerol oxidation reaction. Tables 1 and 2 present activity data for the two Au–C samples. A

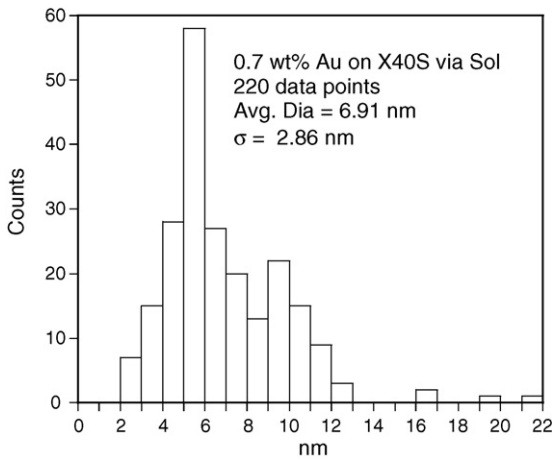

Fig. 8. Particle size histogram for the 0.7 wt% Au on activated carbon prepared by PVA sol.

Table 1
Catalytic activity data for 0.74 wt% Au/C prepared by sputtering

	t (min)			
	15	30	60	120
Conversion	81.0	90.3	98.2	–
Selectivity				
Glycerate	41.6	40.6	37.5	
Oxalate	6.5	6.5	6.9	
Tartronate	11.6	14.7	19.2	
Glycolate	36.6	34.7	32.7	
Hydroxypyruvate	3.7	3.5	3.7	

Reaction conditions: 0.3 M with NaOH/glycerol ratio = 4 mol/mol, glycerol/gold ratio = 1000 mol/mol, pO_2 = 3 atm, and T = 50 °C.

Table 2
Catalytic activity data for 0.70 wt% Au/C prepared by PVA sol

	t (min)			
	15	30	60	120
Conversion	40.3	65.8	86.4	97.5
Selectivity				
Glycerate	57.0	57.9	58.1	56.2
Oxalate	3.1	2.8	2.5	2.5
Tartronate	12.0	13.5	14.8	17.9
Glycolate	24.2	22.3	21.0	20.3
Hydroxypyruvate	3.7	3.5	3.5	3.1

Reaction conditions: 0.3 M with NaOH/glycerol ratio = 4 mol/mol, glycerol/gold ratio = 1000 mol/mol, pO_2 = 3 atm, and T = 50 °C.

reaction scheme for the oxidation of glycerol has been presented [23]. It is believed that this reaction can follow two pathways leading to the formation of a number of stable intermediate products (or their salts). Path A converts glycerol to hydroxypyruvic acid (hydroxypyruvate), and then glycolic acid (glycolate) can be formed. Path B converts glycerol to glyceric acid (glycerate), then tartronic acid (tartronate), followed by oxidative decarboxylation to the oxalate.

Comparing the data in Tables 1 and 2, we can derive several conclusions. First, we can conclude that the smaller supported catalysts prepared by sputtering are almost twice as active than the larger ones prepared via PVA sol. Second, we can see that the sputter prepared catalysts are less selective for the formation of glycerate and tartronate (path B) than the PVA-sol catalysts, 46.7% products versus 74.1% products. Finally, we see that the sputtered catalysts convert nearly three times the amount of glycerol to oxalate as the PVA-sol catalysts, demonstrating again the enhanced activity of the smaller sputtered catalysts. These results are consistent with previous reports in the literature indicating that larger particles are significantly less reactive but more selective for the oxidation of glycerol [16]. While no gold leaching was observed for these samples the recyclability and the long-term stability of these catalysts was not evaluated but will be in subsequent studies.

4. Conclusions

This paper has demonstrated the utility of the magnetron sputtering technique towards the formation of supported

catalytic gold nanoparticles. Using this technique we were able to synthesize two different catalyst systems. The Au/WO_3 catalyst, which cannot be prepared using conventional chemical methods due to WO_3's very low isoelectric point, is reported for the first time. We also demonstrated that this system is catalytically active for the oxidation of carbon monoxide. In a second example, we have prepared the smallest gold particles supported on carbon that have been reported. Catalytic activity measurements of Au/C from different synthesis methods show that smaller gold nanoparticles are less selective but more active for the oxidation of glycerol.

Acknowledgments

The authors would like to thank Mrs. Tamara Keever of Oak Ridge National Laboratories Chemical Sciences Division for assistance with ICP. The WO_3 support material was graciously provided by the H. C. Stark Chemical company. LP and AV are grateful for financial support from the Auricat EU network (HPRN-CT-2002-00174). The research performed at Oak Ridge National Laboratory was sponsored by the U.S. Department of Energy's Office of Basic Energy Sciences, Division of Materials Science and Engineering, under contract DE-AC05-00OR 22725, with ORNL, managed & operated by UT-Battelle, LLC.

References

[1] M. Mavrikakis, P. Stoltze, J.K. Nørskov, Cat. Let. 64 (2000) 101.
[2] M. Haruta, J. New Mater. Electrochem. Sys. 7 (2004) 163.
[3] G.C. Bond, D.T. Thompson, Cat. Rev. -Sci. Eng. 41 (1999) 319.
[4] G.C. Bond, Catal. Today 72 (2002) 5.
[5] M.B. Cortie, E. van der Lingen, Mater. Forum 26 (2002) 1.
[6] A. Wolf, F. Schüith, Appl. Catal. A: Gen. 226 (2002) 1.
[7] M. Haruta, CATTECH 6 (2002) 102.
[8] F. Moreau, G.C. Bond, A.O. Taylor, J. Catal. 231 (2005) 105.
[9] C.L. Bianchi, S. Biella, A. Gervasini, L. Prati, M. Rossi, Cat. Let. 85 (2002) 91.
[10] M.M. Schubert, S. Hackenberg, A.C. van Veen, M. Muhler, V. Plzak, R.J. Behm, J. Catal. 197 (2001) 113.
[11] M. Comotti, W.-C. Li, B. Spliethoff, F. Schüth, J. Am. Chem. Soc. 128 (2006) 917.
[12] N. Weiher, E. Bus, L. Delannoy, C. Louis, D.E. Ramaker, J.T. Miller, J.A. van Bokhoven, J. Catal. 240 (2006) 100.
[13] S.E.S. El Wakkad, H.A. Rizk, J. Phys. Chem. 61 (1957) 494.
[14] G.A. Parks, Chem. Rev. 65 (1965) 177.
[15] S. Carrettin, P. McMorn, P. Johnston, K. Griffin, G.J. Hutchings, Chem. Commun. 2002 (2002) 696.
[16] F. Porta, L. Prati, J. Catal. 224 (2004) 397.
[17] G.M. Veith, A.R. Lupini, S.J. Pennycook, G.W. Ownby, N.J. Dudney, J. Catal. 231 (2005) 151.
[18] G.M. Veith, A.R. Lupini, S.J. Pennycook, N.J. Dudney, in: E. Gaigneaux (Ed.), Studies in Surface Science and Catalysis, 2006, p. 71.
[19] L. Prati, G. Martra, Gold Bull. 32 (1999) 96.
[20] P.D. Nellist, M.F. Chisholm, N. Dellby, O.L. Krivanek, M.F. Murfitt, Z.S. Szilagyi, A.R. Lupini, A. Borisevich, W.H. Sides Jr., S.J. Pennycook, Science 305 (2004) 1741.
[21] S.J. Pennycook, P.D. Nellist, in: D.G. Rickerby, U. Valdrè, G. Valdrè (Eds.), Impact of Electron and Scanning Probe Microscopy on Materials Research, Kluwer Academic Publishers, Dordrect, The Netherlands, 1999 p. 166.
[22] P.D. Nellist, S.J. Pennycook, Adv. Img. Elect. Phys. 113 (2000) 147.
[23] N. Dimitratos, J.A. Lopez-Sanchez, D. Lennon, F. Porta, L. Prati, A. Villa, Cat. Let. 108 (2006) 147.